Biosensors and Bioelectronics 105 (2018) 103–108

Contents lists available at ScienceDirect

Biosensors and Bioelectronics

journal homepage: www.elsevier.com/locate/bios

An electrochemical biosensor for microRNA-196a detection based on cyclic enzymatic signal amplification and template-free DNA extension reaction with the adsorption of methylene blue

Jing Guo, Changjing Yuan, Qi Yan, Qiuyue Duan, Xiaolu Li, Gang Yi*

Key Laboratory of Medical Diagnostics of Ministry of Education, Department of Laboratory Medicine, Chongqing Medical University, Chongqing 400016, PR China

ARTICLE INFO

Keywords:
Electrochemical biosensor
MicroRNA
Cyclic enzymatic signal amplification
Template-free DNA extension reaction
Methylene blue

ABSTRACT

A simple and sensitive electrochemical biosensor was developed for microRNA-196a detection, which is of important diagnostic significance for pancreatic cancer. It was based on cyclic enzymatic signal amplification (CESA) and template-free DNA extension reaction. In the presence of microRNA-196a, duplex-specific nuclease (DSN) catalyzed the digestion of the 3′-PO_4 terminated capture probe (CP), resulting in the target recycling amplification. Meanwhile, the 3′-OH terminal of CP was exposed. Then, template-free DNA extension reaction was triggered by terminal deoxynucleotidyl transferase (TdT), producing amounts of single-stranded DNA (ssDNA). After ssDNA absorbed numerous methylene blue (MB), an ultrasensitive electrochemical readout was obtained. Based on this dual amplification mechanism, the proposed biosensor exhibited a high sensitivity for detection of microRNA-196a down to 15 aM with a linear range from 0.05 fM to 50 pM. This biosensor displayed high specificity, which could discriminate target microRNAs from one base mismatched microRNAs. It also showed good reproducibility and stability. Furthermore, it was successfully applied to the determination of microRNA-196a in plasma samples. In conclusion, with the excellent analytical performance, this biosensor might have the potential for application in clinical diagnostics of pancreatic cancer.

1. Introduction

MicroRNAs (miRNAs) are single-stranded non-protein-coding RNAs with approximately a length of 22 nucleotides. They play important roles in regulating gene expression (Bartel, 2004; Eulalio et al., 2008). Research evidence showed that aberrant expression of miRNAs has the high correlation with the occurrence of various cancers (Kent and Mendell, 2006; Ventura and Jacks, 2009). Recently, pancreatic cancer has become one of the most common causes of cancer-related death. Three independent groups have reported that the levels of several specific miRNAs (miR-21, miR-196a, miR-155 and so on) in humans peripheral blood are closely related to pancreatic cancer (Huang et al., 2016; Liu et al., 2012; Wang et al., 2009). These strongly suggest that miRNAs have great potentials to work as promising biomarkers for the diagnosis of pancreatic cancer. However, miRNAs are high sequence homology, small size, and low expression levels in plasma (Li et al., 2016). Thus, it is quite challenging to sensitively and specifically analyze miRNAs. Therefore, it is urgent to develop a sensitive approach for miRNAs detection.

Electrochemical sensors have the advantages of high sensitivity, low cost and few sample consumption (Liu et al., 2016). They have gained wide attention in miRNAs detection. To achieve high sensitivity, amplification strategies are usually used in biosensors, such as hybridization chain reaction (HCR) (Jie et al., 2017), rolling circle amplification (RCA) (Zhang et al., 2015b) and catalytic hairpin assembly (CHA) (Zhang et al., 2016). Nevertheless, these strategies often involve complex probe design process or complicated DNA sequence analysis. Thus, a kind of cyclic enzymatic signal amplification (CESA) catalyzed by duplex-specific nuclease (DSN) has been developed owing to its simplicity and high efficiency (Yin et al., 2012). In CESA, the specific cleavage preference of DSN for DNA in DNA-RNA hybrid duplexes is mainly used (Lu et al., 2016). During the digestion process, RNA can be reused through repeated cycles of hybridization, digestion and dissociation. As a result, the responding signal can be amplified significantly (Zhang et al., 2015a). More importantly, the nuclease has a wonderful capability to discriminate perfectly matched from slightly mismatched (even one base mismatch) short duplexes (Shagin et al., 2002). Despite many advantages, CESA suffers a relatively low sensitivity (Ren et al., 2013), which may counteract the analytical performance of biosensors.

* Corresponding author.
E-mail address: yigang666@126.com (G. Yi).

https://doi.org/10.1016/j.bios.2018.01.036
Received 1 November 2017; Received in revised form 6 January 2018; Accepted 17 January 2018
Available online 31 January 2018
0956-5663/

Template-free DNA extension reaction is another amplification method popular used in different sensing strategy. This amplification method is assisted by terminal deoxynucleotidyl transferase (TdT). TdT is a template-independent DNA polymerase (Liu et al., 2014). It can catalyze the sequential addition of deoxyribonucleoside 5′-triphosphates (dNTP) at 3′-OH group of DNA to produce a long single-stranded DNA (ssDNA) structure directly (Shen et al., 2015). Since the template is not required in the extension reaction, the reaction system can be easily designed and operated. As a simple, direct and efficient isothermal amplification, it has become an essential step in the process of miRNA sensors design for nucleic acid detection and quantification. However, to the best of our knowledge, no electrochemical biosensor has been developed with the use of DSN assisted CESA and template-free DNA extension reaction.

Various metal nanoparticles are widely used, such as gold nanoparticles (AuNPs) (Saleh et al., 2017a), silver nanoparticles (AgNPs) (Alshalalfeh et al., 2016; Al-Shalalfeh et al., 2017; Saleh et al., 2016, 2017b) and copper nanoparticles (CuNPs) (Chi et al., 2017). Although these metal nanoparticles could generate excellent signals, they usually need a complicated process of fabrication. This may limit their application to some extent. Methylene blue (MB) was a redox complex. Compared with circular nanoparticles, Mb can bind specifically to guanine bases on ssDNA easily due to its unique planar structure (Nordin et al., 2016). And that it can be used without the complicated preparation. However, so far as we know, reports of MB used as a redox indicator for template-free DNA extension reaction are very rare.

To develop a simple and sensitive electrochemical biosensor for miRNA-196a detection, we combined CESA with template-free DNA extension reaction. In this cascade signal amplification strategy, only one nucleotide sequence was used. In addition, MB was properly used as an electroactive redox indicator in our strategy. What's more, because of the simple principle and probe design, the detection process is easy to implement, and the cost is reduced to a certain degree. Compared with other methods, our strategy exhibits superior specificity and lower detection limit. Due to the excellent analytical performance of this method, it may become a potential alternative tool for detection of miRNA in biomedical research and early clinical diagnosis.

2. Experimental section

2.1. Chemicals and materials

All HPLC-purified DNA oligonucleotides and miRNAs were synthesized by Sangon Biotech Co. (Shanghai, China), and their base sequences were listed in Table S1. 6-mercapto-1-hexanol (MCH) was purchased from Sigma (St. Louis, MO, USA). DSN and 10 × DSN master buffer (500 mM Tris-HCl, 50 mM $MgCl_2$, 10 mM DTT, pH 8.0) were obtained from Evrogen Joint Stock Company (Moscow, Russia). TdT, 10× terminal transferase reaction buffer (500 mM Potassium Acetate, 200 mM Tris-acetate, 100 mM Magnesium Acetate, pH 7.9) and 2.5 mM $CoCl_2$ were purchased from New England Biolabs. Ltd. (USA). Deoxyguanosine triphosphate (dGTP), deoxycytidine triphosphate (dCTP), deoxythymidine triphosphate (dTTP), deoxyadenosine triphosphate (dATP) and methylene blue (MB) were obtained from Sangon Biotech Co. (Shanghai, China). Ultrapure water obtained from a Millipore water purification system (18.2 MΩ, MilliQ, Millipore) was used in all experiments. The ultrapure water used in miRNA-related experiments was treated with DEPC.

Several buffers were used in this study: Saline sodium citrate (SSC) buffer as the hybridization buffer (pH 7.4) contained 30 mM Sodium Citrate and 300 mM NaCl. 0.1 M phosphate buffered solution (PBS, pH 7.4) containing 0.1 M Na_2HPO_4, 0.1 M NaH_2PO_4, and 0.1 M $MgCl_2$ was served as the working buffer to perform electrochemical measurements. The washing buffer was PBS (0.01 M, pH 7.4) containing 0.05% (w/v) Tween-20.

2.2. Apparatus

All electrochemical assay measurements were performed on the CHI660D electrochemical workstation (Shanghai Chen Hua Instruments, Shanghai, China). A conventional three-electrode system was employed: Ag/AgCl electrode as reference, platinum wire as auxiliary and gold disk electrode (3 mm in diameter, 5 mm in length) as the working electrode (GaossUnion Technology Co., Ltd, Wuhan, China). Gel images were recorded on an imaging system (Bio-Rad Laboratories, USA). All measurements were carried out at room temperature.

2.3. Preparation of sensors

The bare gold disk electrode with a diameter of 3 mm was polished with 0.05 mm alumina slurry to a mirror-like finish and treated ultrasonically in ultrapure water for 5 min. The electrode was then soaked in freshly prepared piranha solution (the mixture of 98% H_2SO_4 and 30% H_2O_2 at a volume ratio of 3:1) for 10 min followed by rinsing thoroughly with ultrapure water to eliminate residual alumina powder. Afterwards, the pretreated electrode was dried at room temperature. Then, the obtained electrode was immersed into 10 μL of 10 μM MCH solution for 20 min. After washing with ultrapure water, 10 μL of 500 nM thiol-modified capture probe (CP) was dropped on the prepared electrode surface. Then, the electrode was incubated for 12 h at 4 °C. The electrochemical biosensor was rinsed with 0.01 M PBS (pH 7.4) containing 0.05% (w/v) Tween-20 and used for the following operation.

2.4. Amplified detection of miRNA

Droplets of 10 μL mixtures containing a series of different concentrations of the miRNA-196a and 0.06 U DSN in 1× DSN master buffer (50 mM Tris-HCl, 5 mM $MgCl_2$, 1 mM DTT, pH 8.0) were incubated with sensors for 100 min at 37 °C. Rinsed with the washing buffer and water, 10 μL of reaction mixture containing 5 U TdT, 4 mM dGTP, 0.8 mM dNTPs (dATP, dCTP and dTTP), 1× terminal transferase reaction buffer (50 mM Potassium Acetate, 20 mM Tris-acetate, 10 mM Magnesium Acetate, pH 7.9) and 0.25 mM $CoCl_2$ was dropped on the electrode surface and incubated at 37 °C for 60 min to form long ssDNA. After washing with PBS and ultrapure water, 10 μL of 0.1 M PBS buffer containing 0.5 mM MB was dropped on the electrode surface for 30 min in the dark. Finally, the electrode was washed with washing buffer. The differential pulse voltammetry (DPV) measurement was performed in the working solution (0.1 M PBS, pH 7.4) with a pulse period of 0.5 s, a pulse width of 0.2 s, a pulse amplitude of 50 mV and potential scan from − 0.4 V to 0 V.

2.5. Native polyacrylamide gel electrophoresis

The dual signal amplification strategy was verified by 8% native polyacrylamide gel electrophoresis (PAGE) in 1× TBE buffer (90 mM Tris-boric acid, 2 mM EDTA, pH 8.0). In this analysis, each sample contained 10 μL of the reaction solution and 2 μL of 6× loading buffer. The concentration of CP was 2 μM. CP was incubated with the same amount of miRNA-196a in the SSC hybridization buffer for 1 h at 37 °C. For CESA, 2 μM CP and 50 pM miRNA-196a was incubated with 0.06 U DSN at 37 °C for 2 h. Template-free DNA extension reaction was obtained by the incubation of the product of CESA, 5 U TdT, 4 mM dGTP and 0.8 mM dNTPs (dATP, dCTP, dTTP) for 1 h at 37 °C. After samples were added into the gel, they were run at 110 V constant voltage at room temperature for 30 min. Then, they were stained by GoldView I Nuclear Staining Dyes for 30 min and detected under UV light. Images were recorded by an imaging system.

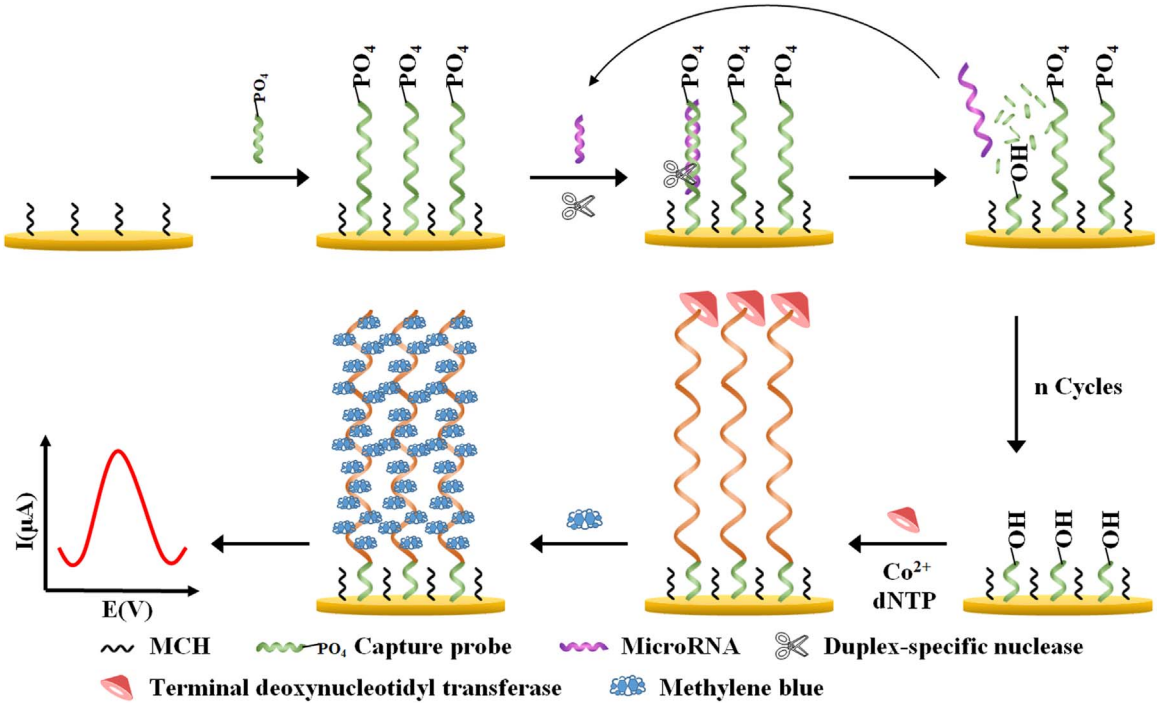

Fig. 1. Schematic illustration of the electrochemical miRNA biosensor based on CESA and template-free DNA extension amplification.

3. Results and discussion

3.1. Design of the electrochemical sensor

The mechanism of the biosensor we proposed for sensitive detection of miRNA is detailed in Fig. 1. MCH was immobilized on the gold electrode surface before the 3′-PO_4 terminated CP was inserted in the interspaces of MCH. This strategy made single-stranded CP standing and uniformly distributed (Josephs and Ye, 2013), which could improve the capture efficiency of the probe. When the target miRNA was added to the electrode, it hybridized with CP to form a CP/miRNA duplex. Once the heteroduplex was formed, the target recognition sequence of the CP was selectively hydrolyzed by DSN and exposed the 3′-OH group. Simultaneously, the recycle of target miRNA generated a great deal of cleaved CP fragments with 3′-OH terminals. In the presence of TdT and dNTP, especially Co^{2+} was added to improve the priming efficiency, the 3′-OH group on the electrode surface triggered sequential DNA extension. Generated substantial long ssDNA specifically adsorbed positively charged MB via guanine bases. Using as the electroactive indicator, MB turned to leucomethylene blue (LB) after oxidization and amplified electrochemical signal were obtained.

3.2. Characterization of the biosensor fabrication

Electrochemical impedance spectroscopy (EIS) and square wave voltammetry (SWV) measurements were effective methods to demonstrate each step of the modification of the working electrode (Zhang et al., 2015c). Thus, they were perfectly used to monitor the layer-by-layer assembly process with the use of $[Fe(CN)_6]^{3-/4-}$ as the redox probe (Sun et al., 2016). EIS measurements were performed from 0.01 to 10^5 Hz with a signal amplitude of 5 mV in 0.4 M KCl containing 0.5 mM $[Fe(CN)_6]^{3-/4-}$. Semicircle diameters of curves equaled to electron-transfer resistance (Ret). As shown in Fig. 2A, an almost straight line (curve a) indicated that the electroactive ions transported easily on the electrode surface, reflecting the excellent electron-transfer capability of the bare gold electrode. Subsequent assembling of MCH led to an increase of Ret (curve b). When CP was self-assembled onto the bare electrode successfully, the Ret (curve c) increased more. Ret (curve d) further increased after the target miRNA was hybridized with the CP. The Ret (curve e) decreased significantly when the biosensor reacted with DSN, which proved the successful implementation of CESA. Afterwards, when template-free DNA extension reaction was finished, the Ret was sharply increased (curve f). SWV for miRNA biosensor detection at different stages were from − 0.1 V to + 0.5 V with a pulse amplitude of 25 mV in 0.4 M KCl containing 0.5 mM $[Fe(CN)_6]^{3-/4-}$. Fig. 2B showed that these results were in a good agreement with those obtained from EIS measurements, in which the peak currents varied with the assembly and reaction processes based on enzymes. All these experimental results proved that the fabrication of the biosensor was implemented successfully.

To prove the feasibility of the strategy, PAGE experiment was carried out. As shown in Fig. 2C, the left side of the gel was loaded with DNA marker (lane 0). When the CP existed alone, it exhibited one band (lane 1). After hybridization with the target miRNA, the mobility of the hybrid was reduced (lane 2). When DSN was added, the band (lane 3) disappeared, because the fragment was too short to appear in the gel after the CP in the hybrid duplex was cleaved by DSN (Lv et al., 2016). A new long trailing band (lane 4) was observed when DNA extension reaction was performed in the presence of TdT and dNTP (Yuan et al., 2014). These results showed that the signal amplification strategy was successful and feasible.

3.3. Amplification performance of the proposed biosensor

To investigate the amplification performance of the proposed method, DPV responses were studied with and without the dual signal amplification strategy under the optimal experimental conditions. As shown in Fig. 3, in the absence of target miRNA, single-stranded CP could not be digested by DSN and there was no 3′-OH terminal for DNA extension. Thus, a small current response (curve a) was obtained due to the little amount of MB absorbed on the CP. In the presence of 50 pM target miRNA (without CESA), small amounts of 3′-OH terminal belonged to miRNA were introduced and triggered DNA extension reaction. Therefore, increased current response (curve b) was observed. However, when DSN was added alone, CESA was performed. Amounts of CP were cleaved on the electrode surface, resulting in decreased

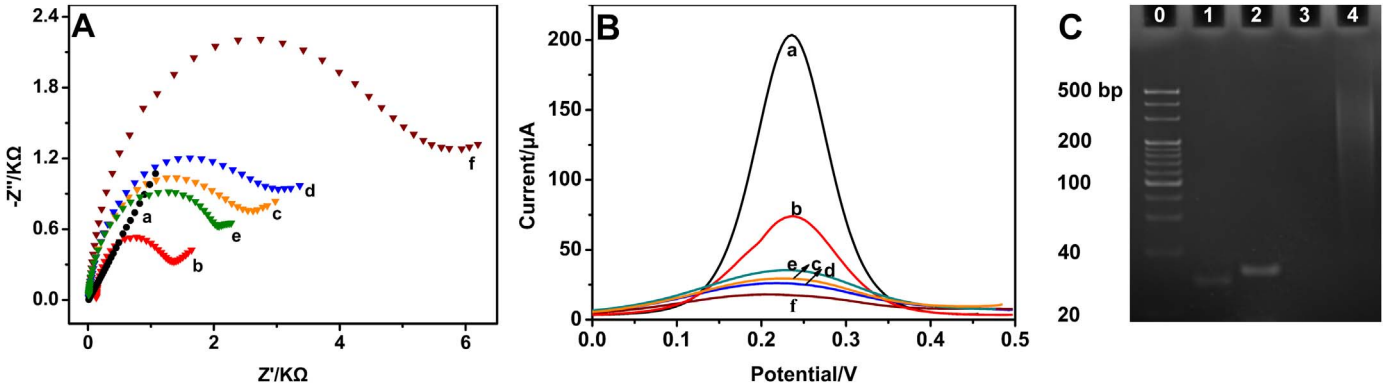

Fig. 2. Characterization of the miRNA biosensor. (A) EIS recorded at different stages: bare gold electrode (a), MCH/Au electrode (b), CP/MCH/Au electrode (c), miRNA/CP/MCH/Au electrode (d), DSN/miRNA/CP/MCH/Au electrode (e), TdT/DSN/miRNA/CP/MCH /Au electrode (f) from 0.01 to 10^5 Hz with a signal amplitude of 5 mV in 0.4 M KCl containing 0.5 mM $[Fe(CN)_6]^{3-/4-}$. (B) SWV for miRNA biosensor at different stages from − 0.1 V to + 0.5 V with a pulse amplitude of 25 mV in 0.4 M KCl containing 0.5 mM $[Fe(CN)_6]^{3-/4-}$. (C) The native PAGE characterization of the prepared biosensor: Line 0: 20 bp DNA marker; Line 1: CP; Line 2: CP hybridized with target miRNA for 1 h at 37 °C; Line 3: mixture of CP, miRNA-196a and DSN incubated for 2 h at 37 °C; Line 4: mixture of line 3, TdT and dNTP with the use of Co^{2+} incubated for 1 h at 37 °C.

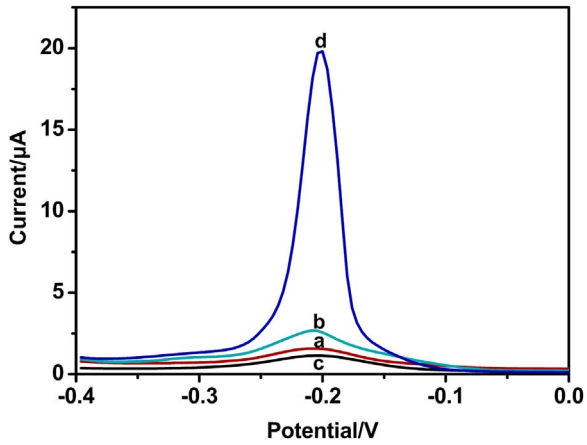

Fig. 3. The DPV responses of 0.5 μM capture probe modified electrode in (a) absence of and (b) presence of 50 pM miRNAs with template-free DNA extension reaction, (c) presence of 50 pM miRNAs with CESA, and (d) presence of 50 pM miRNAs with CESA and template-free DNA extension reaction (6 U/mL DSN, 500 U/mL TdT, 4 mM dGTP, 0.8 mM dNTPs). Pulse period; 0.5 s, pulse width; 0.2 s, pulse amplitude; 50 mV, and potential scan; from − 0.4 V to 0 V.

absorption amount of MB. Hence, the current response decreased (curve c). After CESA and template-free DNA extension reaction occurred, a large amount of long ssDNA generated and absorbed substantial MB, causing the enhanced electrochemical signal. Thus, a remarkable current peak (curve d) was obtained. The experimental results clearly showed that the dual signal amplification strategy was successful and remarkable.

3.4. Optimization of experimental conditions

To obtain the optimal analytical performance, several experimental parameters were optimized. In these experiments, when one parameter changed, other conditions were controlled the same as those in Fig. 3. CESA could be affected by two important parameters, the concentration of DSN and the incubation time. As shown in Fig. S1A, the peak current response was plotted against the amount of DSN in 10 μL CESA mixture from 0.02 U to 0.10 U. The signal was increased with the increase of DSN concentration until the enzyme amount exceeded 0.06 U. Thus, 0.06 U was chosen in further experiments. As shown in Fig. S1B, the incubation time of the CESA process was examined from 40 min to 120 min. The signal increased with the increase of incubation time, and then reached a plateau when it exceeded 100 min. Therefore, 100 min of incubation time was employed in the subsequent experiments.

The concentration of TdT and reaction time were crucial factors affecting the products of template-free DNA extension reaction. Fig. S1C demonstrated the effect of the concentration of TdT in 10 μL TdT extension mixture on the DPV current response from 1 U to 6 U. The maximum signal was achieved when the concentration was 5 U and then tended to decline. Thus, 5 U was employed in further experiments. Also, the incubation time of the extension reaction was investigated. As shown in Fig. S1D, DPV response enhanced with the increase of incubation time, and then almost kept stable when it exceeded 60 min. Therefore, 60 min was chosen as the optimum reaction time for template-free DNA extension reaction.

As MB adsorption was depended on the numbers of guanine bases on ssDNA, the number of guanine bases influenced the signal amplification directly. Thus, the concentration of dGTP and concentration ratio of dGTP and dNTPs (dATP, dCTP, dTTP) was investigated. With the increasing dGTP concentration, the signal enhanced and finally reached a plateau after 4 mM (Fig. S1E). Thus, 4 mM of dGTP was chosen for the subsequent experiments. With the increasing concentration ratio of dGTP and dNTPs, the signal enhanced and finally reached the stable value at 5:1 (Fig. S1F). Therefore, 5:1 was adopted as the optimal concentration ratio.

3.5. Sensitivity of the designed biosensor

Under the optimal conditions, the dependence of the current response upon the various concentrations of the target miRNA was investigated. As shown in Fig. 4A, the peak current increased with the increasing concentration of target miRNA. Fig. 4B displayed a linear relationship between the enhanced signal intensity and the logarithm of target miRNA concentration from 0.05 fM to 50 pM with a correlation coefficient of 0.9987. The regression equation was $\Delta I(\mu A) = 4.044 + 2.865 \lg C$ (fM) (ΔI represented the peak current difference between the absence and presence of the target miRNA, C was the concentration of target miRNA, n = 3). The detection limit of the proposed biosensor was estimated to be 15 aM according to the rule that signal was equivalent to 3 times the standard deviation of the blanks.

The proposed method was compared with other reported methods (Table 1). Among these methods, HCR/nanostructure (Liu et al., 2015) and RCA/magnetic nanoparticle (Yu et al., 2017) used nanoparticles, sequences or template in their biosensors, which made the design time-consuming and complicated. Mismatched CHA (Zhang et al., 2015c) and CHA/enzyme (Shuai et al., 2016) both required complex sequence analysis. Cyclic enzymatic amplification method (CEAM) (Wang et al., 2014) was simple, but the detection limit of our research was much lower than its detection. Compared with other reported methods, our method was simple and exhibited high sensitivity. Such an attractive

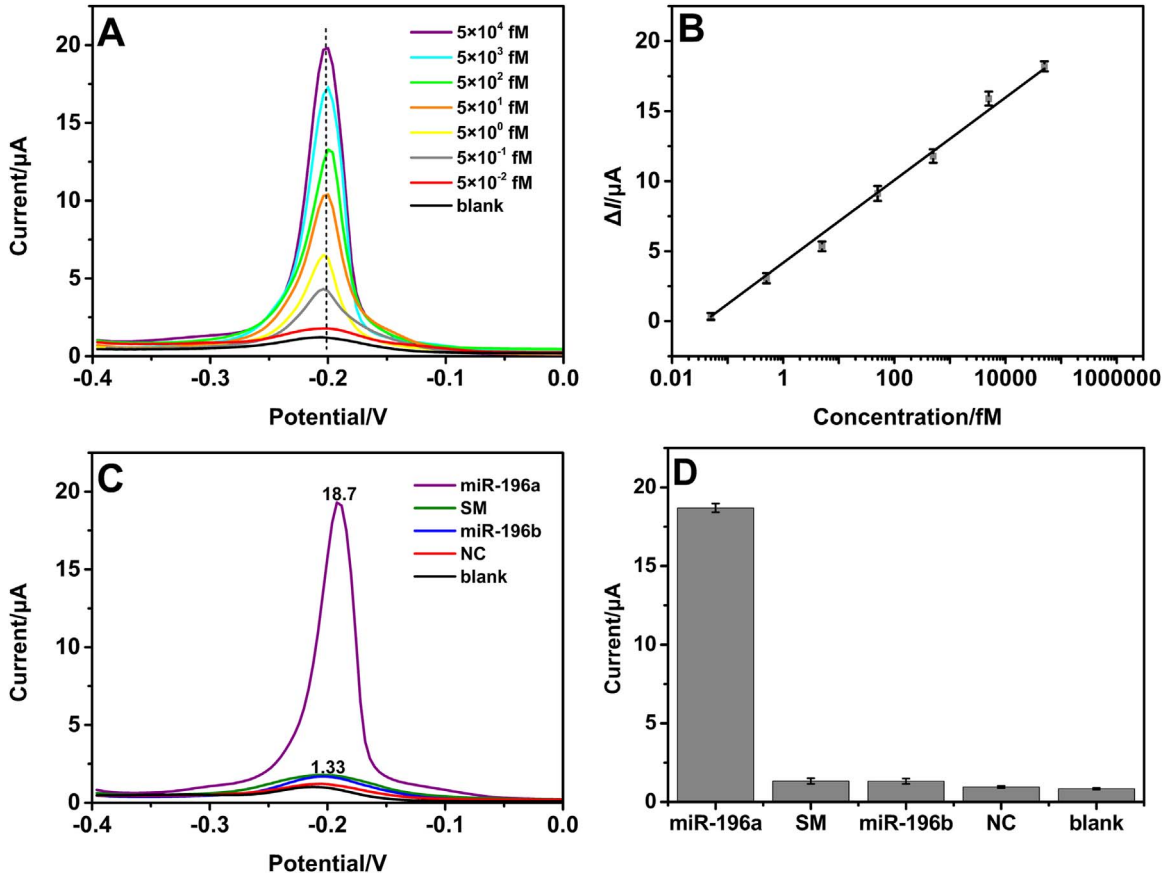

Fig. 4. (A) Typical DPV curves responding to different concentration of target miRNA. Pulse period; 0.5 s, pulse width; 0.2 s, pulse amplitude; 50 mV, and potential scan; from − 0.4 V to 0 V. (B) Plot of DPV peak current vs. logarithm of target miRNA concentration from 0.05 fM to 50 pM. (C) Typical DPV curves and (D) DPV peak currents respectively respond to 50 pM target miRNA (a), SM (b), miR-196b (c), NC (d), and blank (e). Pulse period; 0.5 s, pulse width; 0.2 s, pulse amplitude; 50 mV, and potential scan; from − 0.4 V to 0 V. The error bars represent standard deviations in three repetitive experiments for each concentration.

Table 1
The comparison of the proposed electrochemical biosensor with other reported methods for miRNA detection.

Amplification strategy	Analytical technique	Linear range	LOD	Reference
HCR/nanostructure	DPV	10 fM to 1.0 nM	1.95 fM	(Liu et al., 2015)
RCA/magnetic nanoparticles	SWV	1.0 fM to 2.0 nM	300 aM	(Yu et al., 2017)
Mismatched CHA	DPV	1.0 pM to 25 nM	600 fM	(Zhang et al., 2015c)
CHA/enzyme	DPV	0.10 fM to 0.10 nM	50.0 aM	(Shuai et al., 2016)
CEAM.	DPV	0.50 fM to 0.10 pM	170 aM	(Wang et al., 2014)
CESA/ template-free DNA extension reaction	DPV	50 aM to 50 pM	15.0 aM	This work

analytical performance of the biosensor we designed was primarily attributed to the mechanism of combining CESA and template-free DNA extension reaction.

3.6. Specificity, reproducibility and stability of the assay

In addition, due to the high sequence homology of miRNAs, it is a great challenge to distinguish miRNA family members (Wark et al., 2008). To investigate the specificity of the proposed biosensor, we challenged the assay with miRNA-196a and other three different synthetic oligonucleotides including single-base mismatched strand (SM), miR-196b and non-complement sequence (NC). As shown in Fig. 4C, the signal intensity for SM (curve b), miR-196b (curve c) and NC (curve d) at the concentration of 50 pM were similar to that of the blank (curve e). However, in the presence of miRNA-196a, there was a remarkable increase in the DPV current (curve a) and showed a response 14.06 times as much as that of the SM (Fig. 4D). Clearly, miRNA-196a could be easily differentiated with other miRNA sequences, revealing the good specificity for the determination of target miRNA.

The reproducibility was carried out by determining the target miRNA at 50 pM and 50 fM with five different biosensors. The relative standard deviation (RSD) of two concentrations were 2.6% and 3.3%, respectively, suggesting the good reproducibility of this method.

To demonstrate the cycling stability of the proposed biosensor, the modified electrode was scanned by cyclic voltammetry (CV) (Madhurantakam et al., 2017; Wu et al., 2016) in the potential range of − 0.2 to 0.8 V at the scan rate of 0.1 V s^{-1} in 0.5 mM $[Fe(CN)_6]^{3-/4-}$ solution for 60 continuous cycle scans (Fig. S2). Compared with the initial peak current, a 1.5% change was observed, indicating the good cycling stability of the proposed biosensor. Meanwhile, the successive stability of the proposed biosensor was evaluated by DPV (Hu et al., 2015) with 50 pM of target miRNA. When the DPV detection was completed, the electrode was washed with PBS for the next test. After 60 DPV measurements, a RSD of 7.4% was obtained (Fig. S3). These

Table 2
Assay results of spiking miR-196a into human plasma by the electrochemical biosensor.

Sample	Added miRNA /fM	Detected miRNA /fM	Recovery (%) (n = 5)	RSD (%)
1	0	Undetectable		
2	0.0500	0.0509	101.8	1.8
3	5.00	4.88	97.60	2.1
4	500	511	102.2	2.8

results demonstrated that our biosensor had an acceptable stability.

3.7. Detection of miR-196a spiked plasma samples

To prove the performance of the fabricated biosensor for detection of miRNA in the blood samples, plasma samples spiked with different concentrations (0.05 fM, 5 fM and 500 fM) of chemically synthesized miR-196a were tested with the use of the strategy we designed. The plasma samples were diluted 100-fold with SSC buffer and the initial concentrations of miR-196a in the plasma samples were undetectable. Recovery values listed in Table 2 ranged from 97.6% to 102.2%, showing that the detection of miR-196a in spiked plasma samples could be achieved with the satisfactory recoveries. These results suggested that the established miRNA biosensor provided a potential analytical tool for the detection of miRNA in real samples.

4. Conclusion

In summary, the proposed ultrasensitive electrochemical biosensor combining cyclic enzymatic signal amplification and template-free DNA extension reaction for signal enhancement was successfully developed. The dual amplification led to an extremely high sensitivity with a detection limit as low as 15 aM. What is more, taking advantage of the exclusive hydrolytic capability of DSN which can discriminate even one base mismatch, our electrochemical sensing strategy exhibited high specificity. Moreover, as a simple designed principle, the feasibility was promising, and the cost was relatively low. Therefore, with these excellent properties of our strategy, the biosensor would provide a great potential for biomedical research and early clinical diagnosis.

Acknowledgments

This work was supported by the Special Fund Project for Key Laboratory of Clinical Laboratory Diagnostics, Chongqing Medical University.

Appendix A. Supporting information

Supplementary data associated with this article can be found in the online version at http://dx.doi.org/10.1016/j.bios.2018.01.036.

References

Al-Shalalfeh, M.M., Onawole, A.T., Saleh, T.A., Al-Saadi, A.A., 2017. Mater. Sci. Eng. 76, 356–364.
Alshalalfeh, M.M., Saleh, T.A., Alsaadi, A.A., 2016. RSC Adv. 6, 75282–75292.
Bartel, D.P., 2004. Cell 116, 281–297.
Chi, B.Z., Liang, R.P., Qiu, W.B., Yuan, Y.H., Qiu, J.D., 2017. Biosens. Bioelectron. 87, 216–221.
Eulalio, A., Huntzinger, E., Izaurralde, E., 2008. Cell 132, 9–14.
Hu, Y., Shen, Q., Li, W., Liu, Z., Nie, Z., Yao, S., 2015. Biosens. Bioelectron. 63, 331–338.
Huang, J., Liu, J., Chen-Xiao, K., Zhang, X., Lee, W.N., Go, V.L., Xiao, G.G., 2016. Biomark. Res. 4, 20.
Jie, G., Tan, L., Zhao, Y., Wang, X., 2017. Biosens. Bioelectron. 94, 243–249.
Josephs, E.A., Ye, T., 2013. ACS Nano 7, 3653–3660.
Kent, O.A., Mendell, J.T., 2006. Oncogene 25, 6188–6196.
Li, D.D., Cheng, W., Yan, Y.Y., Zhang, Y., Yin, Y.B., Ju, H.X., Ding, S.J., 2016. Talanta 146, 470–476.
Liu, H.Y., Bei, X.Q., Xia, Q.T., Fu, Y., Zhang, S., Liu, M.C., Fan, K., Zhanng, M.Z., Yang, Y., 2016. Microchim. Acta 183, 297–304.
Liu, J., Gao, J., Du, Y., Li, Z., Ren, Y., Gu, J., Wang, X., Gong, Y., Wang, W., Kong, X., 2012. Int. J. Cancer 131, 683–691.
Liu, L., Song, C., Zhang, Z., Yang, J., Zhou, L., Zhang, X., 2015. Biosens. Bioelectron. 70, 351–357.
Liu, Z., Li, W., Nie, Z., Peng, F., Huang, Y., Yao, S., 2014. Chem. Commun. 50, 6875–6878.
Lu, W.J., Chen, Y.P., Liu, Z., Tang, W.B., Feng, Q., Sun, J.S., Jiang, X.Y., 2016. ACS Nano 10, 6685–6692.
Lv, W., Zhao, J., Bo, S., Bo, L., Wen, M., Liu, J., 2016. Biosens. Bioelectron. 83, 250–255.
Madhurantakam, S., Jayanth, B.K., Balaguru Rayappan, J.B., Krishnan, U.M., 2017. Biosens. Bioelectron. 87, 832–841.
Nordin, N., Yusof, N.A., Abdullah, J., Radu, S., Hushiarian, R., 2016. Biosens. Bioelectron. 86, 398–405.
Ren, Y., Deng, H., Shen, W., Gao, Z., 2013. Anal. Chem. 85, 4784–4789.
Saleh, T.A., Al-Shalalfeh, M.M., Al-Saadi, A.A., 2016. Sci. Rep. 6, 32185.
Saleh, T.A., Al-Shalalfeh, M.M., Onawole, A.T., Al-Saadi, A.A., 2017a. Vib. Spectrosc. 90, 96–103.
Saleh, T.A., Al-Shalalfeh, M.M., Al-Saadi, A.A., 2017b. Mater. Res. Bull. 91, 173–178.
Shagin, D.A., Rebrikov, D.V., Kozhemyako, V.B., Altshuler, I.M., Shcheglov, A.S., Zhulidov, P.A., 2002. Genome Res. 12, 1935–1942.
Shen, Q., Han, L., Fan, G., Zhang, J.R., Jiang, L., Zhu, J.J., 2015. Anal. Chem. 87, 4949–4956.
Shuai, H.L., Huang, K.J., Xing, L.L., Chen, Y.X., 2016. Biosens. Bioelectron. 86, 337–345.
Sun, Y., Ren, Q., Liu, B., Qin, Y., Zhao, S., 2016. Biosens. Bioelectron. 78, 7–13.
Ventura, A., Jacks, T., 2009. Cell 136, 586–591.
Wang, J., Chen, J., Chang, P., LeBlanc, A., Li, D., Abbruzzesse, J.L., Frazier, M.L., Killary, A.M., Sen, S., 2009. Cancer Prev. Res. 2, 807–813.
Wang, M., Fu, Z., Li, B., Zhou, Y., Yin, H., Ai, S., 2014. Anal. Chem. 86, 5606–5610.
Wark, A.W., Lee, H.J., Corn, R.M., 2008. Angew. Chem. Int. Ed. 47, 644–652.
Wu, Y., Sheng, K., Liu, Y., Yu, Q., Ye, B., 2016. Anal. Chim. Acta 1–8.
Yin, B.C., Liu, Y.Q., Ye, B.C., 2012. J. Am. Chem. Soc. 134, 5064–5067.
Yu, N., Wang, Z., Wang, C.C., Han, J., Bu, H.Y., 2017. Anal. Chim. Acta 962, 24–31.
Zhang, C.H., Tang, Y., Sheng, Y.Y., Wang, H., Wu, Z., Jiang, J.H., 2016. Chem. Commun. 52, 13584–13587.
Zhang, J., Wu, D., Chen, Q., Chen, M., Xia, Y., Cai, S., Zhang, X., Wu, F., Chen, J., 2015a. Analyst 140, 5082–5089.
Zhang, P., Wu, X., Yuan, R., Chai, Y., 2015b. Anal. Chem. 87, 3202–3207.
Zhang, Y., Yan, Y., Chen, W., Cheng, W., Li, S., Ding, X., Li, D., Wang, H., Ju, H., Ding, S., 2015c. Biosens. Bioelectron. 68, 343–349.